Journal of the Ceramic Society of Japan 121 [2] 169-175 2013 Paper

Preparation and NO reduction property of apatite-type $ALa_9Si_6O_{26}$ (A = Li, Na, K) supported Pt catalyst

Atsunori ONO, Sumio KATO,† Tatsuya NARUMI, Yuji ADACHI, Masataka OGASAWARA, Takashi WAKABAYASHI,* Yuunosuke NAKAHARA* and Shinichi NAKATA

Department of Applied Chemistry, Graduate School of Engineering and Resource Science, Akita University, 1–1 Tegatagakuen-machi, Akita 010–8502, Japan

***Catalysts Strategic Division, Mitsui Mining & Smelting Co., Ltd., 1013–1 Ageoshimo, Ageo, Saitama 362–0025, Japan**

Apatite-type $ALa_9Si_6O_{26}$ (A = Li, Na, K) were prepared by solid state reaction method. The hexagonal unit cell volumes of $ALa_9Si_6O_{26}$ increased with increasing ionic radii of alkali metal ions, indicating that the alkali metal ions were incorporated into the apatite-type lattice. The specific surface areas of $ALa_9Si_6O_{26}$ were less than 1 m^2/g. X-ray photoelectron spectroscopy measurement showed that Pt species on as-prepared catalysts were highly oxidized. Reduction temperature of Pt oxides on the catalyst for temperature-programmed reduction by H_2 was decreased by substitution of alkali metal ion at La site in the apatite-type silicate. For C_3H_6–NO–O_2 reaction, $Pt/NaLa_9Si_6O_{26}$ catalyst exhibited a maximum NO conversion of 42%, the highest among $Pt/ALa_9Si_6O_{26}$ catalysts. The temperature for maximum NO conversion over $Pt/NaLa_9Si_6O_{26}$ catalyst was lower than that over Pt/γ-Al_2O_3 catalyst under the same reaction condition. The temperature of 50% C_3H_6 conversion for C_3H_6–O_2 reaction over $Pt/ALa_9Si_6O_{26}$ catalysts increased in the sequence of A = K < A = Na < A = Li. In addition, C_3H_6 oxidation activity was suppressed by presence of CO_2 and NO on the catalyst. These results suggest that the basic sites on the apatite-type support affect the catalytic activities of $Pt/ALa_9Si_6O_{26}$ catalysts for C_3H_6–NO–O_2 and C_3H_6–O_2 reaction.

Key-words : Apatite-type silicate, NO reduction, Pt catalyst, Alkali metal, C_3H_6 oxidation

[Received July 2, 2012; Accepted October 10, 2012]

1. Introduction

Reduction of NO by hydrocarbons (HC) is an efficient way to remove NO from automobile exhaust gas. Platinum, palladium and rhodium (PGM: platinum group metal) catalysts are widely used for NO reduction, and a large number of studies on the catalysts have been reported.[1)–10)] For PGM catalysts, γ-Al_2O_3 is often used as a support.[5),10)–12)] Recently, it is found that addition of alkali metals to γ-Al_2O_3 supported PGM catalyst increases catalytic activity for NO reduction. Vernoux et al. investigated the influence of Na on catalytic activity of Pt/γ-Al_2O_3 with various loading rates (0.12–5 wt%).[13)] They showed that the catalytic activity of Pt/γ-Al_2O_3 catalyst for C_3H_6–NO–CO–O_2 reaction was improved by addition of Na. The temperatures for 50% C_3H_6 conversion and for the maximum NO conversion to N_2 and N_2O were shifted toward lower temperatures. Konsolakis et al. showed that the NO reduction on Pt/γ-Al_2O_3 catalyst was promoted by addition of Li (0.16–4.7 wt%), K (0.9–8.8 wt%), Rb (1.9–15.5 wt%) and Cs (3.0–24.0 wt%) for C_3H_6–NO reaction.[14)] In this case, NO conversion and N_2 selectivity were increased by addition of alkali metals. It seems that the catalytic activity of PGM catalyst for NO reduction is promoted by basicity of the catalyst.

In our previous study, it was found that the catalytic activity of the apatite-type $La_{9.33}Si_6O_{26}$ supported Pt catalyst was higher than that of γ-Al_2O_3 supported Pt catalyst.[15)] Furthermore, the catalytic activity of the apatite-type lanthanum silicate supported Pt catalyst was promoted by substitution of alkaline earth metals (Ca, Sr, Ba) at La site.[16)] These results suggested that the basicity of the support is an important factor in controlling the catalytic activities.

The alkali metals have low electronegativity compared with lanthanum and alkaline earth metals. Therefore, it is presumed that the basicity of the apatite-type lanthanum silicate support is increased by substitution of alkali metal ions, leading to improvement of the catalytic activities of apatite-type silicates supported Pt catalyst. In this study, we prepared alkali metals containing lanthanum apatite-type silicate, $ALa_9Si_6O_{26}$ (A = Li, Na, K), supported Pt catalysts and evaluated their catalytic activity for NO reduction using C_3H_6 as a reductant. In order to investigate the effects of the alkali metal substitution to the apatite-type silicate support on the reaction including C_3H_6, NO and O_2 as reactants, the catalytic activities for C_3H_6–NO–O_2, C_3H_6–O_2 and NO–O_2 reactions were also evaluated.

2. Experimental

2.1 Catalyst preparation

The apatite-type silicates containing lanthanum and alkali metal ions, $ALa_9Si_6O_{26}$ (A = Li, Na, K), were synthesized by the solid state reaction method. The powders of La_2O_3, SiO_2 and alkali metal carbonate (A_2CO_3) were used as starting materials. The molar ratios of the starting materials were A_2CO_3:La_2O_3:SiO_2 = x:4.5:6, where, x = 0.65 for A = Li, Na and x = 1 for A = K. These materials were mixed in ethanol by ball-milling. Excess alkali metal carbonates were added to compensate for the loss due to evaporation of alkali metal compounds at high temperature. The mixtures were pressed into pellets of 10 mm diameter and heated at 800–1200°C for 6–12 h in air with intermediate grindings. The synthesis conditions for $ALa_9Si_6O_{26}$ are listed in **Table 1**. The alkali metal free apatite-type lanthanum

† Corresponding author: S. Kato; E-mail: katos@gipc.akita-u.ac.jp

Table 1. Synthesis conditions of $ALa_9Si_6O_{26}$ (A = Li, Na, K)

$ALa_9Si_6O_{26}$	Synthesis condition
A = Li	800°C 12 h and 1100°C 12 h
A = Na	800°C 12 h and 1100°C 24 h
A = K	800°C 6 h and 1200°C 12 h

silicate, $La_{9.33}Si_6O_{26}$ was synthesized by the sol–gel method reported by Tao et al.[17] Tetraethyl orthosilicate (TEOS) and La_2O_3 were used as starting materials. The mixed solution including 4.0 g of TEOS, 93 cm^3 of C_2H_5OH and 3 cm^3 of CH_3COOH was stirred at room temperature to obtain a clear solution. Then, 4.52 g of La_2O_3, 90 cm^3 of distilled water and 10 cm^3 of 13 mol/dm^3 HNO_3 were added into the solution and dissolved completely by stirring. The obtained clear solution was heated at 80°C for 6 h, resulting in a sol solution, and an amorphous gel was obtained by drying the solution at 90°C for 12 h. The precursor was obtained by heating the amorphous gel at 600°C for 7 h in air. Apatite-type $La_{9.33}Si_6O_{26}$ was obtained by heating the precursor at 1250°C for 48 h in air with three intermediate regrindings. Catalysts loaded with 1 mass % of Pt were prepared by impregnating $ALa_9Si_6O_{26}$ and $La_{9.33}Si_6O_{26}$ with $Pt(NH_3)_2(NO_2)_2$ aqueous solution and heating at 600°C for 3 h in air.

2.2 Characterization

Phase identification of the silicates and catalysts was performed by powder X-ray diffraction (XRD) using Cu Kα radiation (40 kV, 40 mA). X-ray diffraction patterns were recorded with a Rigaku Ultima IV X-ray diffractometer. The chemical compositions of the $ALa_9Si_6O_{26}$ were determined by inductively coupled plasma atomic emission spectrometry (ICP-AES), using an SII NanoTechnology Inc. SPS 3500-DD. The specific surface areas of the $ALa_9Si_6O_{26}$ and $La_{9.33}Si_6O_{26}$ powders were evaluated by the Brunauer-Emmet-Teller (BET) method from N_2 adsorption isotherm at −196°C, using a Bel Japan BELSORP-miniII. The chemical states of Pt on the catalyst surface were evaluated by X-ray photoelectron spectroscopy (XPS), using a JEOL JPS-9000SX system with Mg Kα radiation and KRATOS AXIS-ULTRA DLD with Al Kα radiation. The binding energy (BE) was calibrated using the C1s line (BE = 285.0 eV).

The dispersion of Pt on the catalysts was evaluated by the CO pulse adsorption method reported by Takeguchi et al.[18] A quartz tube reactor was loaded with 0.5 g of catalyst. The catalyst was heated to 400°C at 10°C/min and held for 10 min in flowing air at 100 cm^3/min. Then, the catalyst was purged with He fed at 100 cm^3/min for 1 min, and then H_2 fed at 100 cm^3/min for 10 min, and thereafter cooled down to 50°C under He atmosphere. Subsequently the catalyst was held at 50°C under switched feed gases. The order of the feed gases was: air (5 min), He (1 min), CO_2 (10 min), He (1 min), H_2 (5 min) and He (5 min), at 100 cm^3/min. The CO pulse adsorption was performed at 50°C. The concentration of CO in the effluent gas was evaluated using a Shimadzu GC-8A gas chromatograph with a thermal conductivity detector (TCD). The reduction properties of Pt on the catalysts were investigated by temperature programmed reduction by H_2 (H_2-TPR). Before the H_2-TPR measurement, the catalyst was heated up to 200°C at 10°C/min and held for 1 h to remove adsorbed water, and then cooled down to room temperature under He atmosphere. Then, the measurement was performed in flowing 6%H_2–He at 50 cm^3/min by heating up to 800°C at 10°C/min. The amounts of H_2 consumption were monitored using a gas analyzer (Canon Anelva M-201GA-DM) with a quadrupole mass spectrometer. The amounts of H_2 consumption for the reduction of Pt on $Pt/La_{9.33}Si_6O_{26}$ catalyst were measured by H_2 pulse reduction. Before the H_2 pulse reduction, the catalyst was heated up to 200°C at 10°C/min and held for 1 h to remove adsorbed water, and then cooled down to room temperature under Ar atmosphere. The measurement was performed in 6%H_2–Ar pulse injection at 25 and 250°C. The concentration of H_2 in the effluent gas was evaluated using a Shimadzu GC-8A gas chromatograph with a TCD.

Table 2. Composition of feed gases for C_3H_6–NO–O_2, C_3H_6–O_2 and NO–O_2 reactions

Gas	Concentration (ppm)		
	C_3H_6–NO–O_2 reaction	C_3H_6–O_2 reaction	NO–O_2 reaction
C_3H_6	1500	1500	—
NO	1000	—	1000
O_2	9000	9000	9000
He	Balance	Balance	Balance

2.3 Evaluation of catalytic activity

The catalytic activity for NO reduction, C_3H_6 oxidation and NO oxidation was evaluated using a fixed bed flow reactor. The catalyst was formed into a pellet and crushed. Then, 0.1 g of catalyst, which had been passed through a 26-mesh sieve but trapped on a 42-mesh sieve, was loaded into a quartz tube reactor of 10 mm diameter. Prior to the reaction, the catalyst was heated at 600°C for 10 min in flowing 1.5%O_2–He gas. The compositions of the feed gases for C_3H_6–NO–O_2, C_3H_6–O_2 and NO–O_2 reactions are shown in **Table 2**. The reactions were carried out at a gas flow rate of 500 cm^3/min (W/F = 0.012 g s/cm^3) in the temperature range of 200 to 600°C. The effluent compositions were analyzed using a Shimadzu GC-14B gas chromatograph with a flame ionization detector (FID) and a Shimadzu NOA-7000 NOx analyzer. To investigate the influence of acidic gas adsorption on catalytic activity, evaluation of catalytic activity for C_3H_6–O_2 reaction was performed after CO_2 adsorption treatment on the catalyst by exposure to 1%CO_2–He gas for 1 h at room temperature.

3. Results and discussion

3.1 Catalyst preparation and characterization

Figure 1(a) shows XRD patterns of $ALa_9Si_6O_{26}$ (A = Li, Na, K) obtained by the solid state reaction method and $La_{9.33}Si_6O_{26}$ obtained by the sol–gel method. The peaks were indexed on the basis of hexagonal unit cell. The molar ratios of La, Si and A in $ALa_9Si_6O_{26}$ are listed in **Table 3**. These ratios are close to stoichiometric composition of $ALa_9Si_6O_{26}$. For A = Li and Na, ratios of (La + A) are 10.15 and 10.19, which are larger than 10, respectively, suggesting presence of small amounts of excess alkali metal on the catalysts. The lattice constants, hexagonal unit cell volumes of $ALa_9Si_6O_{26}$ and ionic radii of alkali metal ions[19] are listed in **Table 4**. The volumes of the apatites increased with increasing ionic radii of alkali metal ions. This result indicates that the alkali metal ions were incorporated into the apatite-type lattice. The weak peaks observed at $2\theta = 26.1$ and 28.7°, for alkali metal free-sample, were assigned to $La_2Si_2O_7$. Figure 1(b) shows XRD patterns of $Pt/ALa_9Si_6O_{26}$ catalysts and $Pt/La_{9.33}Si_6O_{26}$ catalyst prepared by the impregnation method. The peaks of apatite-type phase were observed after Pt loading, and no apparent peaks of Pt derived phase, such as Pt, PtO and PtO_2, were detected, suggesting that no large crystalline Pt compounds

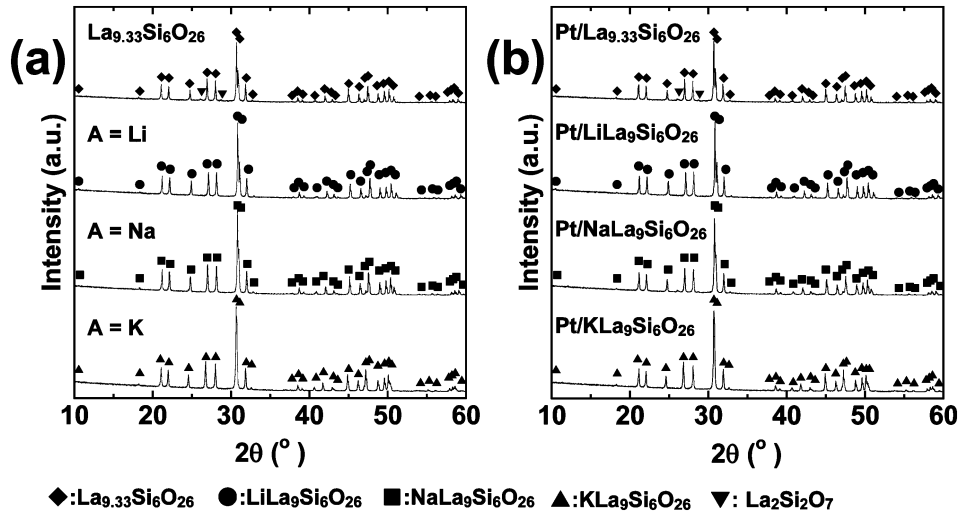

Fig. 1. XRD patterns of (a) $ALa_9Si_6O_{26}$ (A = Li, Na, K), $La_{9.33}Si_6O_{26}$ and (b) apatite-type silicate supported Pt catalysts.

Table 3. Molar ratios of La, Si and A (A = Li, Na, K) in $ALa_9Si_6O_{26}$

$ALa_9Si_6O_{26}$	Molar ratios (−)		
	La	Si*	A
A = Li	9.16	6.00	0.99
A = Na	9.15	6.00	1.04
A = K	8.89	6.00	1.00

*Molar ratios of Si are fixed at 6.00.

Table 4. Lattice constants, unit cell volume of $ALa_9Si_6O_{26}$ (A = Li, Na, K) and ionic radius of A^+

$ALa_9Si_6O_{26}$	Lattice constants		Unit cell volume	Ionic radius of A^{+}*
	a (nm)	c (nm)	V (nm^3)	(nm)
A = Li	0.96901(7)	0.71524(5)	0.5816	0.106
A = Na	0.96940(10)	0.71880(7)	0.5850	0.132
A = K	0.97291(5)	0.72442(3)	0.5930	0.165

*8-coordination environment.

Table 5. Specific surface area of supports and CO/Pt of $Pt/ALa_9Si_6O_{26}$ (A = Li, Na, K) and $Pt/La_{9.33}Si_6O_{26}$ catalysts

Catalyst	Specific surface area (m^2/g)	CO/Pt
$Pt/La_{9.33}Si_6O_{26}$	0.7	0.05
$Pt/LiLa_9Si_6O_{26}$	0.4	0.02
$Pt/NaLa_9Si_6O_{26}$	0.4	0.06
$Pt/KLa_9Si_6O_{26}$	0.4	0.04

formed on the catalysts. Specific surface areas of supports and CO/Pt for catalysts are listed in **Table 5**. All of the specific surface areas for the apatite-type silicate supports were small (0.4–0.7 m^2/g), because the apatite-type silicate supports were synthesized at high temperature (1100–1250°C). The CO/Pt for the $Pt/ALa_9Si_6O_{26}$ and $Pt/La_{9.33}Si_6O_{26}$ catalysts was 0.02, 0.06, 0.04 and 0.05 for A = Li, Na, K and $Pt/La_{9.33}Si_6O_{26}$, respectively. These values indicate that the amounts of exposed Pt atoms on catalyst surface were small, and no significant difference of Pt dispersion was observed among the catalysts. The XPS spectra of the Pt 4f region for the as-prepared apatite-type silicate supported Pt catalysts are shown in **Fig. 2**. The Pt 4f spectra for all the catalysts could be fit to two doublets. The

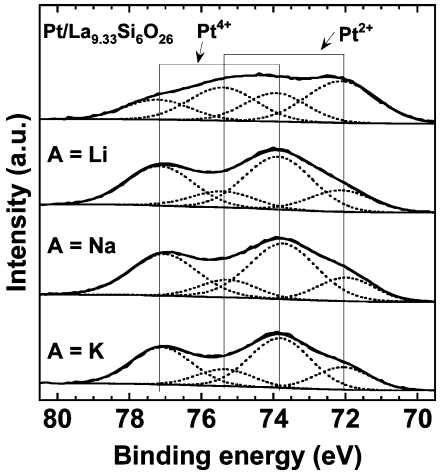

Fig. 2. Pt 4f XPS spectra of $Pt/ALa_9Si_6O_{26}$ (A = Li, Na, K) and $Pt/La_{9.33}Si_6O_{26}$ catalysts.

Pt $4f_{7/2}$ peaks were observed at 72.0–72.1 and 73.7–73.9 eV. The binding energies of the Pt $4f_{7/2}$ peaks are listed in **Table 6**. Hecq et al. reported that the binding energies of Pt $4f_{7/2}$ were 72.3 eV for PtO and 73.6 eV for PtO_2 in the case of oxygen-platinum compounds.[20] From their results, the two doublets of Pt 4f spectra for the catalysts were assigned to Pt^{2+} and Pt^{4+} species. The molar fractions of Pt^{2+} and Pt^{4+} calculated by curve fitting of the spectra are listed in Table 6. The fraction of Pt^{4+} was more than 70% for $Pt/ALa_9Si_6O_{26}$ catalysts, and 37% for $Pt/La_{9.33}Si_6O_{26}$, indicating that Pt on these catalysts was highly oxidized. **Figure 3** shows the H_2-TPR curves of the apatite-type silicate supported Pt catalysts. Hydrogen consumption peak was observed at 94, 96, 87 and 383°C for A = Li, Na, K and $Pt/La_{9.33}Si_6O_{26}$ catalysts. The reduction temperature for $Pt/La_{9.33}Si_6O_{26}$ was much higher than that for $Pt/ALa_9Si_6O_{26}$, and broad H_2 consumption was observed in the temperature range of 100–300°C. The amounts of H_2 consumption for Pt reduction on $Pt/La_{9.33}Si_6O_{26}$ catalyst at 25 and 250°C were measured by H_2 pulse reduction. Hydrogen consumption was less than 0.1, and 1.05 μmol/g-cat. at 25 and 250°C, respectively. **Figure 4** shows XPS spectra of the Pt 4f region for $Pt/La_{9.33}Si_6O_{26}$ after H_2 pulse reduction at 25 and 250°C. The Pt $4f_{7/2}$ peaks for $Pt/La_{9.33}Si_6O_{26}$

Table 6. Binding energy of Pt $4f_{7/2}$ and relative peak area for $Pt/ALa_9Si_6O_{26}$ (A = Li, Na, K) and $Pt/La_{9.33}Si_6O_{26}$ catalysts

Catalyst	Binding energy of $4f_{7/2}$ (eV)	Relative peak area (%)	Assignment
$Pt/La_{9.33}Si_6O_{26}$	72.1	63	Pt^{2+}
	73.9	37	Pt^{4+}
$Pt/LiLa_9Si_6O_{26}$	72.0	28	Pt^{2+}
	73.9	72	Pt^{4+}
$Pt/NaLa_9Si_6O_{26}$	72.0	25	Pt^{2+}
	73.7	75	Pt^{4+}
$Pt/KLa_9Si_6O_{26}$	72.1	29	Pt^{2+}
	73.8	71	Pt^{4+}

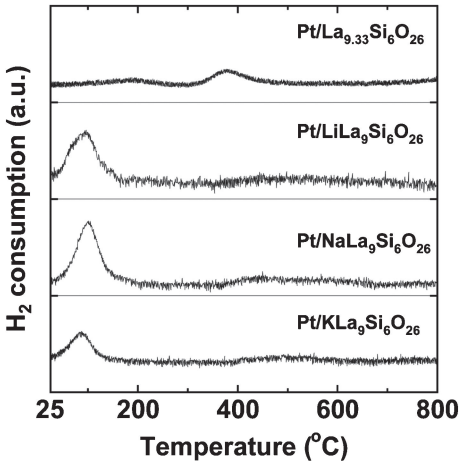

Fig. 3. H_2-TPR curves of $Pt/ALa_9Si_6O_{26}$ (A = Li, Na, K) and $Pt/La_{9.33}Si_6O_{26}$ catalysts.

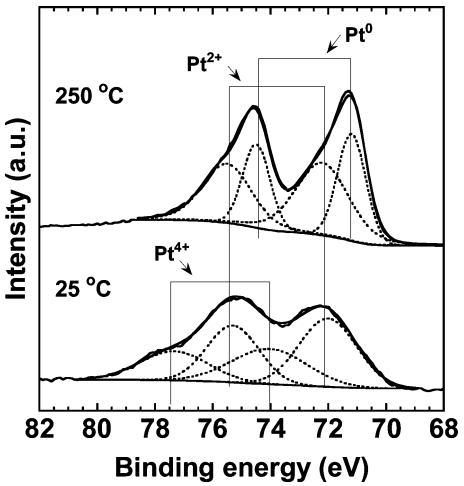

Fig. 4. Pt 4f XPS spectra of $Pt/La_{9.33}Si_6O_{26}$ catalyst after H_2 pulse reduction at 25 and 250°C.

after H_2 pulse reduction at 25°C were observed at 72.0 and 74.0 eV, which could be assigned to Pt^{2+} and Pt^{4+}, respectively. On the other hand, the peaks for $Pt/La_{9.33}Si_6O_{26}$ after H_2 pulse reduction at 250°C were observed at 71.2 and 72.2 eV, which were assigned to Pt^0 and Pt^{2+}, respectively. These results indicated that the Pt oxides on $La_{9.33}Si_6O_{26}$ were not reduced below 25°C, and Pt oxides partially reduced in the temperature range of 25–250°C.

The H_2-TPR results of $Pt/ALa_9Si_6O_{26}$ catalysts indicate that the reduction temperature of Pt oxides on the catalysts was decreased by substitution of alkali metal ion at La site in the apatite-type silicate support. In our previous study, H_2-TPR measurement was performed for $Pt/La_8A'_2Si_6O_{26}$ (A′ = Ca, Sr, Ba)[16] under the same condition. Hydrogen consumption peaks observed at 95 and 89°C for A′ = Sr and Ba. These temperatures were close to those observed in the case of $Pt/ALa_9Si_6O_{26}$ catalysts. On the other hand, H_2 consumption peak was observed at 145°C for A′ = Ca, which is higher than that for A′ = Sr and Ba. From these results, it is presumed that the reduction temperature of Pt oxides was affected by basicity of the apatite-type silicate support, but the difference of effect on lowering the reduction temperature among $Pt/ALa_9Si_6O_{26}$ catalysts is small.

3.2 Catalytic activity

Figure 5(a) shows temperature dependence of NO conversion for C_3H_6–NO–O_2 reaction over $Pt/ALa_9Si_6O_{26}$ (A = Li, Na, K) and $Pt/La_{9.33}Si_6O_{26}$ catalysts in the range of 200–600°C. The maximum NO conversion of $Pt/ALa_9Si_6O_{26}$ catalysts decreased in the sequence of A = Na (42%) > A = Li (35%) > $Pt/La_{9.33}Si_6O_{26}$ (29%) > A = K (23%) and the temperatures for maximum NO conversion were 350, 275, 350 and 325°C for A = Li, Na, K and $Pt/La_{9.33}Si_6O_{26}$ respectively. This result suggests that the substitution of alkali metal ion at La site in apatite-type silicate support affects NO reduction behavior of the $Pt/ALa_9Si_6O_{26}$ and $Pt/La_{9.33}Si_6O_{26}$ catalysts for C_3H_6–NO–O_2 reaction. In our previous study, Pt/γ-Al_2O_3 exhibited a maximum NO conversion of 46% at 325°C,[21] under the same reaction condition. Although the specific surface area of $Pt/NaLa_9Si_6O_{26}$ catalyst (0.4 m^2/g) was smaller than that of Pt/γ-Al_2O_3 catalyst (159 m^2/g), the maximum NO conversion for $Pt/NaLa_9Si_6O_{26}$ catalyst was comparable to that of Pt/γ-Al_2O_3 catalyst. Burch et al. performed kinetics measurements for C_3H_6–NO–O_2 reaction over Pt/SiO_2 and Pt/Al_2O_3. They proposed that C_3H_6 adsorption and formation of carbonaceous species occur on reduced Pt surface during the reaction, and that oxidized Pt is inactive for NO dissociation.[1),22)] This suggests that the chemical state and reduction property of Pt species affect the catalytic behavior for C_3H_6–NO–O_2 reaction. The higher Pt reduction temperature of $Pt/La_{9.33}Si_6O_{26}$ would be one of reason for the lower activity below 275°C compared with $Pt/ALa_9Si_6O_{26}$ (A = Li, Na, K). On the other hand, no significant difference was observed in the chemical state (Fig. 2) and reduction property (Fig. 3) of Pt species on the $Pt/ALa_9Si_6O_{26}$ catalysts. Therefore, it is suggested that the C_3H_6 adsorption and formation of carbonaceous species over Pt on $Pt/ALa_9Si_6O_{26}$ catalysts are not dominant factors causing difference of catalytic activities among the catalysts for C_3H_6–NO–O_2 reaction.

In the case of catalytic NO reduction by hydrocarbon in the presence of O_2, it is also known that NO_2 is formed by NO oxidation as one of the reactive intermediates.[23),24)] To investigate the influence of the apatite-type silicate supports on NO_2 formation, catalytic activities for the NO–O_2 reaction over $Pt/ALa_9Si_6O_{26}$ and $Pt/La_{9.33}Si_6O_{26}$ catalysts were evaluated. **Figure 6** shows temperature dependence of NO conversion into NO_2 over the catalysts and Pt/γ-Al_2O_3 catalyst in the range of 200–600°C. All of the maximum NO conversions over $Pt/ALa_9Si_6O_{26}$ and $Pt/La_{9.33}Si_6O_{26}$ catalysts were less than 9% at 450°C. On the other hand, Pt/γ-Al_2O_3 exhibited higher maximum conversion of 17% at 400°C. Thus, no significant difference was observed for NO oxidation properties among $Pt/ALa_9Si_6O_{26}$ and $Pt/La_{9.33}Si_6O_{26}$ catalysts. These results suggest

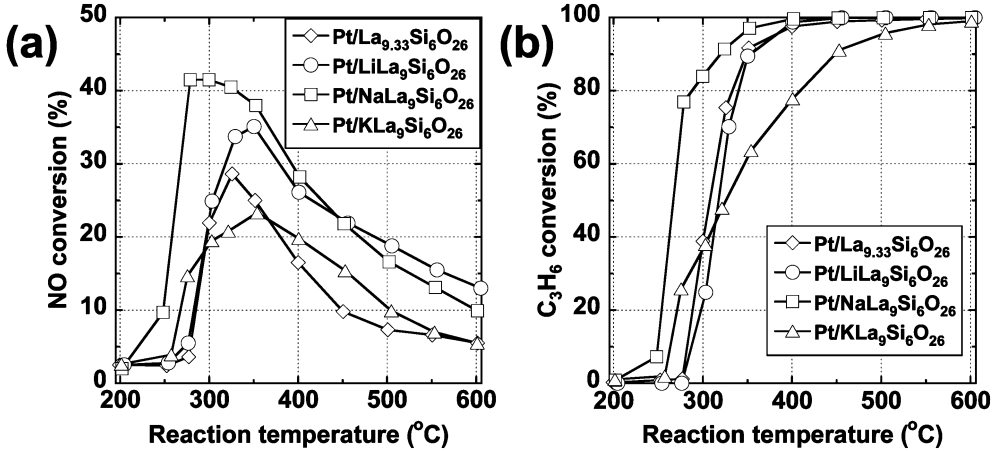

Fig. 5. Temperature dependences of (a) NO and (b) C_3H_6 conversions for C_3H_6–NO–O_2 reaction over $Pt/ALa_9Si_6O_{26}$ (A = Li, Na, K) and $Pt/La_{9.33}Si_6O_{26}$ catalysts.

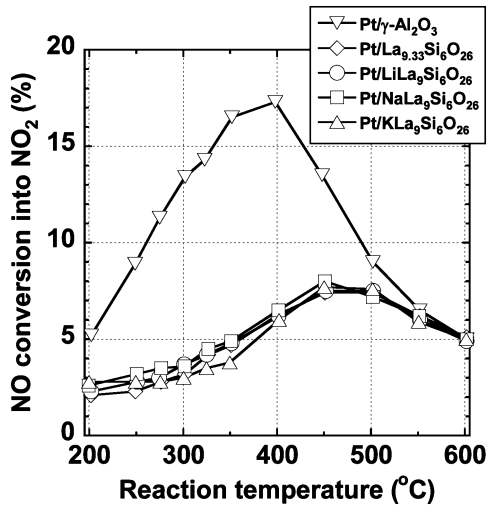

Fig. 6. Temperature dependence of NO conversion for NO–O_2 reaction over $Pt/ALa_9Si_6O_{26}$ (A = Li, Na, K), $Pt/La_{9.33}Si_6O_{26}$ and Pt/γ-Al_2O_3 catalysts.

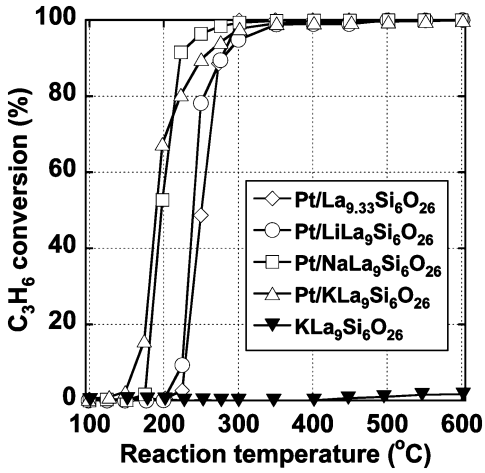

Fig. 7. Temperature dependence of C_3H_6 conversion for C_3H_6–O_2 reaction over $Pt/ALa_9Si_6O_{26}$ (A = Li, Na, K), $Pt/La_{9.33}Si_6O_{26}$ catalysts and $KLa_9Si_6O_{26}$.

that the alkali metal ion substitution at La site in the apatite-type silicate supports has no effect on the catalytic activity for NO oxidation.

In order to investigate the effect of the apatite-type silicate supports on C_3H_6 containing reaction, catalytic activity for C_3H_6–O_2 reaction of $Pt/ALa_9Si_6O_{26}$, $Pt/La_{9.33}Si_6O_{26}$ and $KLa_9Si_6O_{26}$ were evaluated. **Figure 7** shows temperature dependence of C_3H_6 conversion for C_3H_6–O_2 reaction over $Pt/ALa_9Si_6O_{26}$, $Pt/La_{9.33}Si_6O_{26}$ catalysts and $KLa_9Si_6O_{26}$ in the range of 100–600°C. Propene conversion increased sharply at 225°C for $Pt/La_{9.33}Si_6O_{26}$ and at 200 and 175°C for $Pt/ALa_9Si_6O_{26}$ (A = Na and K), respectively. This result indicates that C_3H_6 oxidation activity was improved by substitution of alkali metal ions at La site in the apatite-type silicate support. The temperatures for 50% conversion of C_3H_6, $T_{50}(C_3H_6)$, for C_3H_6–O_2 reaction over $Pt/ALa_9Si_6O_{26}$ and $Pt/La_{9.33}Si_6O_{26}$ catalysts are listed in **Table 7**. The $T_{50}(C_3H_6)$ for C_3H_6–O_2 reaction decreased in the sequence of $Pt/La_{9.33}Si_6O_{26}$ > A = Li > A = Na > A = K, which agrees with the decreasing order of the electronegativity of lanthanum and alkali metals. The catalytic performance of $KLa_9Si_6O_{26}$ without Pt loading was also investigated as shown in Fig. 7. The C_3H_6 conversion over $KLa_9Si_6O_{26}$ was less than 2% below

Table 7. $T_{50}(C_3H_6)$ for C_3H_6–O_2 reactions

Catalyst	$T_{50}(C_3H_6)$ (°C)	
	Fresh	After CO_2 adsorption treatment
$Pt/La_{9.33}Si_6O_{26}$	251	255
$Pt/LiLa_9Si_6O_{26}$	240	264
$Pt/NaLa_9Si_6O_{26}$	197	217
$Pt/KLa_9Si_6O_{26}$	190	251

600°C, indicating that C_3H_6 oxidation occurred over Pt on the $Pt/KLa_9Si_6O_{26}$ catalyst. As described above, no difference of chemical state and reduction property of Pt were observed among $Pt/ALa_9Si_6O_{26}$ catalysts. Therefore, it is suggested that the basicity of apatite-type silicate supports affect the C_3H_6 activation over the supports. Wakabayashi et al. investigated the oxidation of hydrocarbon and the reduction of NO by hydrocarbon species over apatite-type $La_{7.33}BaYSi_6O_{25.5}$ supported Pt catalyst.[25] They performed infrared (IR) spectroscopy measurement for $La_{7.33}BaYSi_6O_{25.5}$ after treatment in flowing 0.25%C_3H_6–N_2 gas, and observed adsorbed carbonous species such as ones completely oxidized to carbonate and partially oxidized to methanol, formaldehyde and dimethylether. In their study, they presumed that the catalytic activity of apatite-type $La_{7.33}BaYSi_6O_{25.5}$

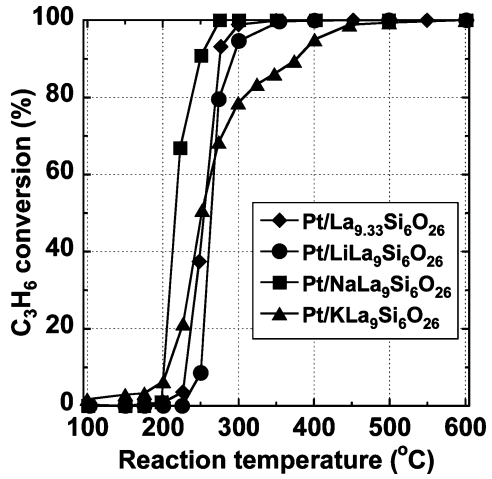

Fig. 8. Temperature dependence of C_3H_6 conversion for C_3H_6–O_2 reaction over $Pt/ALa_9Si_6O_{26}$ (A = Li, Na, K) and $Pt/La_{9.33}Si_6O_{26}$ catalysts after CO_2 adsorption treatment.

supported Pt catalyst for NO reduction by C_3H_6 was affected by the adsorbed form of oxidized carbonous species on $La_{7.33}BaYSi_6O_{25.5}$. In the case of $Pt/ALa_9Si_6O_{26}$ catalysts, basic sites on the apatite-type silicate supports would affect the formation of the carbonous species, resulting in difference of the catalytic activity.

In order to confirm the contribution of the basic sites on the supports, the influence of acidic gases such as CO_2 and NO on catalytic activity of $Pt/ALa_9Si_6O_{26}$ and $Pt/La_{9.33}Si_6O_{26}$ catalysts was investigated. **Figure 8** shows temperature dependence of C_3H_6 conversion for C_3H_6–O_2 reaction over $Pt/ALa_9Si_6O_{26}$ and $Pt/La_{9.33}Si_6O_{26}$ catalysts after CO_2 adsorption treatment in the range of 100–600°C. The values of $T_{50}(C_3H_6)$ for C_3H_6–O_2 reaction over the catalysts are listed in Table 7. The $T_{50}(C_3H_6)$ increased +24, +20, +61 and +4°C for $Pt/ALa_9Si_6O_{26}$ (A = Li, Na, K) and $Pt/La_{9.33}Si_6O_{26}$, respectively, in comparison with the catalysts without the CO_2 adsorption treatment. Propene oxidation activity of A = K was affected more strongly by CO_2 adsorption compared with A = Li and Na. These results indicate that the C_3H_6 oxidation was suppressed by the adsorbed CO_2. As described above, Pt on the catalysts was active site of C_3H_6 oxidation, but it is known that CO_2 is not adsorbed on Pt. Therefore, the suppression of the C_3H_6 oxidation would be caused by prevention of reactive intermediate formation owing to the basic sites on apatite-type silicate supports being covered with the acidic gas.

The influence of NO as an acidic gas, on catalytic activity of $Pt/ALa_9Si_6O_{26}$ and $Pt/La_{9.33}Si_6O_{26}$ catalysts was investigated by comparison between the C_3H_6 conversions for C_3H_6–O_2 reaction (Fig. 7) and C_3H_6–NO–O_2 reaction (Fig. 5). Although the concentrations of C_3H_6 and O_2 in the reaction gases for both reactions were the same, $T_{50}(C_3H_6)$ for C_3H_6–NO–O_2 reaction was higher than that for C_3H_6–O_2 reaction for all catalysts. For example, $T_{50}(C_3H_6)$ of $Pt/La_{9.33}Si_6O_{26}$ catalyst, 308°C, for C_3H_6–NO–O_2 reaction was higher than that for C_3H_6–O_2 reaction, 215°C. This result indicates that the C_3H_6 oxidation was suppressed by presence of NO. In the case of C_3H_6–NO–O_2 reaction, NO adsorption on basic sites of the apatite-type silicate supports would occur, resulting in degradation of catalytic activity for C_3H_6 oxidation. As shown in Fig. 5(a), NO reduction performance of $Pt/KLa_9Si_6O_{26}$, was lower than that of $Pt/LiLa_9Si_6O_{26}$ and $Pt/NaLa_9Si_6O_{26}$. This would be due to strong adsorption of NO on the basic sites, resulting in suppression of C_3H_6 oxidation.

The present work suggests that C_3H_6 activation occurs at basic sites on the support of $Pt/ALa_9Si_6O_{26}$ catalysts, resulting in the promotion of the catalytic activity for C_3H_6–NO–O_2 reaction, and that the basicity of the apatite-type silicate support is the controlling factor of catalytic activity for the reaction. Further spectroscopic investigation such as IR is necessary to clarify formation of intermediates for C_3H_6–NO–O_2 and C_3H_6–O_2 reaction on $Pt/ALa_9Si_6O_{26}$ catalysts.

4. Conclusion

Apatite-type $ALa_9Si_6O_{26}$ (A = Li, Na, K) supported Pt catalysts were prepared and investigated for their catalytic activity for C_3H_6–NO–O_2, C_3H_6–O_2 and NO–O_2 reactions. For C_3H_6–NO–O_2 reaction, $Pt/NaLa_9Si_6O_{26}$ catalyst exhibited the highest maximum NO conversion at the lowest temperature among $Pt/ALa_9Si_6O_{26}$ catalysts.

Catalytic activity of apatite-type silicate supported Pt catalyst for C_3H_6 oxidation was improved by substitution of alkali metal ions at La site in the apatite-type silicate supports. However, C_3H_6 oxidation on apatite-type silicate supported Pt catalysts was suppressed by presence of acidic gases such as CO_2 and NO. From these results, it seems that the reaction intermediate formed over basic sites on the apatite-type silicate support, resulting in enhancement of the catalytic activity. On the other hand, adsorption of CO_2 and NO on the basic site would inhibit formation of the intermediates. Therefore, optimization of basicity of the support would be necessary for improving the catalytic activity for C_3H_6–NO–O_2 reaction.

Acknowledgements This work was partly supported by Grant-in-Aid for Scientific Research (C) (23510089) from Japan Society for Promotion of Science (JSPS).

References

1) R. Burch, J. P. Breen and F. C. Meunier, *Appl. Catal., B*, 39, 283–303 (2002).
2) Z. Zhang, M. Chen, Z. Jiang and W. Shangguan, *J. Hazard. Mater.*, 193, 330–334 (2011).
3) S. Satokawa, J. Shibata, K. Shimizu, A. Satsuma, T. Hattori and T. Kojima, *Chem. Eng. Sci.*, 62, 5335–5337 (2007).
4) R. Bruch and P. J. Millington, *Catal. Today*, 29, 37–42 (1996).
5) S.-C. Shen and S. Kawi, *J. Catal.*, 213, 241–250 (2003).
6) J. Li, J. Hao, L. Fu, T. Zhu, Z. Liu and X. Cui, *Appl. Catal., A*, 265, 43–52 (2004).
7) S. E. Golunski, H. A. Hatcher, R. R. Rajaram and T. J. Truex, *Appl. Catal., B*, 5, 367–376 (1995).
8) V. G. Papadakis, C. A. Pliangos, I. V. Yentekakis, X. E. Verykios and C. G. Vayenas, *Catal. Today*, 29, 71–75 (1996).
9) J. K. Lampert, M. S. Kazi and R. J. Farrauto, *Appl. Catal., B*, 14, 211–223 (1997).
10) G. Corro, J. L. G. Fierro, R. Montiel, S. Castillo and M. Moran, *Appl. Catal., B*, 46, 307–317 (2003).
11) F.-Y. Chang, M.-Y. Wey and J.-C. Chen, *J. Hazard. Mater.*, 156, 348–355 (2008).
12) R. J. Wu, T. Y. Chou and C. T. Yeh, *Appl. Catal., B*, 6, 105–116 (1995).
13) P. Vernoux, A.-Y. Leinekugel-Le-Cocq and F. Gaillard, *J. Catal.*, 219, 247–257 (2003).
14) M. Konsolakis and I. V. Yentekakis, *Appl. Catal., B*, 29, 103–113 (2001).
15) S. Kato, T. Yoshizawa, N. Kakuta, S. Akiyama, M. Ogasawara, T. Wakabayashi, Y. Nakahara and S. Nakata, *Res. Chem. Intermed.*, 34, 703–708 (2008).

16) A. Ono, M. Abe, S. Kato, M. Ogasawara, T. Wakabayashi, Y. Nakahara and S. Nakata, *Appl. Catal., B*, 103, 149–153 (2011).
17) S. Tao and J. T. S. Irvine, *Mater. Res. Bull.*, 36, 1245–1258 (2001).
18) T. Takeguchi, S. Manabe, R. Kikuchi, K. Eguchi, T. Kanazawa, S. Matsumoto and W. Ueda, *Appl. Catal., A*, 293, 91–96 (2005).
19) R. D. Shannon, *Acta Crystallogr., Sect. A: Cryst. Phys., Diffr., Theor. Gen. Crystallogr.*, 32, 751–767 (1976).
20) M. Hecq, A. Hecq, J. P. Delrue and T. Robert, *J. Less-Common Met.*, 64, 25–37 (1979).
21) A. Ono, Y. Takahashi, S. Kato, M. Ogasawara, T. Wakabayashi, Y. Nakahara and S. Nakata, *Res. Chem. Intermed.*, 37, 1225–1230 (2011).
22) R. Burch and T. C. Watling, *Catal. Lett.*, 43, 19–23 (1997).
23) R. Bruch and T. C. Watling, *J. Catal.*, 169, 45–54 (1997).
24) M. D. Amiridis, K. L. Roberts and C. J. Pereira, *Appl. Catal., B*, 14, 203–209 (1997).
25) T. Wakabayashi, S. Kato, Y. Nakahara, M. Ogasawara and S. Nakata, *Catal. Today*, 164, 575–579 (2011).